Influence of Si substitution on the reactivity of α-Tricalcium Phosphate

Mariana Motisuke[1*], Gemma Mestres[2], Caroline O. Renó[1], Raúl G. Carrodeguas[3], Cecília A. C. Zavaglia[4] and Maria-Pau Ginebra[5]

[1] Bioceramics Laboratory – Science and Technology Institute, UNIFESP, 12231-280, São José dos Campos, SP, Brazil

[2] Engineering Sciences Dpt., Uppsala University, Box 534, 751 21 Uppsala, Sweden.

[3] Department of Ceramics, Institute of Ceramics and Glass (ICV), CSIC, Kelsen 5, 28049 Madrid, Spain

[4] Labiomec – Mechanical Engineering School – State University of Campinas, 13083-860, Campinas, SP, Brazil

[5] Engineering Sciences and Metallurgy Dpt., Technical University of Catalonia, Diagonal 647, 08028 Barcelona, Spain.

* Corresponding Author:

Mariana Motisuke

330 Talim Street - Vila Nair

São José dos Campos, SP - Brazil

 Zip Code: 12231-280

Tel.: +55 12 3309-95

Fax: +55 12 3921-8857

motisuke@unifesp.br

Abstract

Silicon substituted calcium phosphates have been widely studied over the last ten years due to their enhanced osteogenic properties. Notwithstanding, the role of silicon on α-TCP reactivity is not clear yet. Therefore, the aim of this work was to evaluate the reactivity and the properties of Si-α-TCP in comparison to α-TCP. Precursor powders have similar properties regarding purity, particle size distribution and specific surface area, which allowed a better comparison of the Si effects on their reactivity and cements properties. Both Si-α-TCP and α-TCP hydrolyzed to a calcium-deficient hydroxyapatite when mixed with water but their conversion rates were different. Si-α-TCP exhibited a slower setting rate than α-TCP, i.e. k_{SSA} for Si-TCP (0.021 g.m^{-2}.h^{-1}) was almost four times lower than for α-TCP (0.072 g.m^{-2}.h^{-1}). On the other hand, the compressive strength of the CPC resulting from fully reacted Si-α-TCP was significantly higher (12.80 ± 0.38 MPa) than that of α-TCP (11.44 ± 0.54 MPa), due to the smaller size of the entangled precipitated apatite crystals.

1. Introduction

Calcium phosphate cements (CPCs) were discovered in the 1980's by Brown, Chown and LeGeros [1,2]. These materials are still actively studied nowadays since CPCs present attractive characteristics such as bioactivity, biocompatibility, osteoconductivity and resorbability [3,4]. Furthermore, CPCs consist on a moldable paste that can be injected into the bone defect using minimally invasive procedures [5–7], with *in vivo* self-setting after a few minutes.

The two most common types of CPCs have been called upon the end-product formed: apatite cement (precipitates at pH > 4.2) and brushite cement (precipitates at pH < 4.2). One of the most common main precursor of apatite cements is α-tricalcium phosphate (α-TCP) [8], which dissolves and precipitates into calcium deficient hydroxyapatite when mixed with water via a cementitious reaction.

Several studies have shown that it is not so easy to obtain a highly pure α-TCP [8–11]. The reason for that has been ascribed to the presence of magnesium impurities in most commercial reagents, a well-established stabilizer of β-TCP, a lower temperature isomorph of TCP [10,12–14]. When Mg^{2+} is present at $\geq$ 4.1 at.% the temperature of $\beta \rightarrow \alpha$ phase transformation can increase from ~1125°C to 1485°C [10,12,15–17]. The temperature of α-TCP synthesis can be reduced by using Mg-free reagents [8,11,18,19]. Cardoso et al. [11] and Motisuke et al. [18,19] succeeded in obtaining α-TCP using impurity-free reagent at a temperatures of 1165ºC and 1300ºC, respectively. On the other hand, Si has been shown to stabilize the α phase down to low temperatures [20,21]. Therefore, another path to reduce the temperature of α-TCP synthesis is by doping α-TCP with silicon (Si-α-TCP). The temperatures for synthesizing Si-α-TCP may vary from 700ºC to 1250º depending on the contents of Mg and/or other impurities [9,22–26].

Si-α-TCP can be obtained by treating at high temperatures a precipitate obtained after mixing calcium nitrate and ammonium phosphate solution at a proper ratio in the presence of ammonia and either colloidal silica or organic silicon compounds [23,27]. An alternative route consists in performing a solid state reaction of mixtures of 1) $CaCO_3$, $CaHPO_4$ or $(NH_4)_2PO_4$, and Ca_2SiO_4 or $CaSiO_3$ [9,28], or 2) β-$Ca_3(PO_4)_2$ and $CaSiO_3$ [29], or 3) HA and SiO_2 [26].

When calcium phosphate cements are prepared from a Si-α-TCP powder some cement properties are altered as compared to its pure counterpart. One example is powder solubility. According to Wei *et.al.* [30], Si increases α-TCP solubility. Mestres *et.al.* [31] verified a faster hydrolysis kinetics, the cement with Si present a similar resistance when compared with the pure, a decrease in cell proliferation and an increased in alkaline phosphatase (ALP) activity, which corresponds to an enhance of cell differentiation. On the other hand, Camiré *et.al.* [28] observed a decrease on powder reactivity and cement mechanical strength and; an increased osteoclastic and osteoblastic activity.

Additionally to the stabilization of α-TCP phase, silicon has been shown to be beneficial for some biological properties such as bone calcification [32]. Si is essential for bone regeneration and therefore can stimulate certain cell activities such as proliferation and differentiation of osteoblasts [26]. Moreover, the bioactivity of a material can be improved by doping it with Si [33–35].

The role of silicon on the reactivity of α-TCP towards the formation of CPCs is not clear yet [19,26,28]. Thus, the aim of this work was: 1) to verify how silicon may influence on the setting reaction of α-TCP bone cement; and 2) to determine how the different reactivity affects the physico-chemical properties of CPCs. The novelty of this work relies on the use of Mg-free precursors for preparing α-TCP and Si-α-TCP [9] and on the attempt to employ

feasible and large scale procedures to promote the production of more accessible bone cements.

2. Materials and methods

2.1 Preparation of TCP powders and bone cement

α-TCP and Si-α-TCP were synthesized by a solid state reaction from the appropriate mixture of lab made Mg-free $CaCO_3$ (Mg wt-% < 0.0180), $CaHPO_4$ (Mg wt-% < 0.0001) and $CaSiO_3$ (Mg wt-% < 0.0001) as described elsewhere [9]. Briefly, $CaCO_3$ and $CaHPO_4$ were mixed to prepare α-TCP, and 2 wt.% of $CaSiO_3$ was included in the mixture to prepare Si-TCP. The powders were calcined for 6 h at 1300ºC for α-TCP and 1200ºC for Si-TCP with a heating rate of 10ºC.min^{-1}. Afterwards, samples were let to cool down inside the furnace without quenching. Finally, the powders were milled in a horizontal ball mill for 48 h using an alumina gridding media of Ø15 mm and ball to powder ratio of 20:1 w/w.

The mixing liquid used in cements was an aqueous solution of Na_2HPO_4 (2.5 wt.%) and $C_6H_8O_7$ (citric acid) (1.5 wt.%) in distilled water. Citric acid was employed as a liquid reducer agent and to promote a more homogeneous setting reaction due to its dispersant effect [36], and Na_2HPO_4 was added to accelerate the setting reaction due to the coomon-ion effect [37]. Cements were prepared by mixing the powder and liquid in a ratio (L/P) of 0.60 mL.g^{-1}. The paste was introduced in Teflon molds (6 mm diameter x 12 mm height), and samples were immersed in 0.9 wt.% of NaCl solution at 37 ºC for setting.

2.2 Characterization of physico-chemical properties

X-Ray Fluorescence (XRF, Philips, MagiX Super Q Version 3.0) was used to evaluate the elemental composition (major and minor components), as well as Ca/P or Ca/(P+Si) ratios of the two TCP powders. X-Ray Diffraction (XRD, Bruker D8 Advance, CuKα, Ni filter, 20 to 40º (2θ), 0.02 º s^{-1}, 40kV and 40mA) was also used for qualitative and quantitative determination of the crystalline phases existing in the starting powders and set cements.

JCPDS files used for phase identification were #09-0348 for α-TCP and #09-0169 for β-TCP. For quantitative determination of β-TCP on the starting powders the internal standard method was employed, in which a diffraction line from the phase quantified (β-TCP) was compared to a diffraction line from a standard (Al_2O_3) mixed with the sample in known proportions [38].

The density of the TCP powders was measured by helium picnometry (Micromeritics, AccuPyc 1330), the specific surface area (SSA) was measured by nitrogen adsorption (Micromeritics, ASAP 2020) according to Brunauer-Emmett-Teller theory and the granulometry of the powder was determined by laser diffraction particle size analysis (Coulter Counter LS 13 320).

The hardening kinetics was monitored by measuring the compressive strength (MTS, Test Star II) of wet samples after different time intervals (2, 4, 8, 24, 72, 120, 168, 360 h), at least 10 cylindrical specimens were tested per condition. After that, samples were immersed in acetone for 2h to stop the setting reaction, and then dried at 100ºC overnight. The crystalline phase composition at each time point was assessed by XRD, (including a JCPDS file #46-0905 for CDHA). The conversion rate was determined by XRD following the procedure proposed by Ginebra et al. [39,40] and Rigo et al. [41]. It is known that the mass fraction of a crystalline material present in a given sample is proportional to their XRD lines intensities. To evaluate the evolution of the setting reaction of the cements studied, the rate of α-TCP conversion (α_t) was evaluated based on the evolution of its mass fraction with time as stated on Equation 1.

$$\alpha_t = \frac{(w_0 - w_\infty) - (w_t - w_\infty)}{(w_0 - w_\infty)}$$ **Equation 1**

Where w_0 is α-TCP mass fraction at initial time (t = 0 h), w_∞ is α-TCP mass fraction after the 168h of setting reaction and w_t is α-TCP mass fraction at a determined time, t. At each time, α-TCP mass fraction was determined after its XRD lines (1 3 2), (1 1 3) and (1 0 7) integrated intensities (Equation 2) and an average value was established.

$$\frac{I_\alpha}{I_{\alpha,0}} = \frac{w_\alpha M_\alpha}{w_{\alpha,0}\left[(M_\alpha - M_{CDHA})(w_\alpha + w_\beta) + M_{CDHA}\right]}$$ **Equation 2**

Where I_α is the integrated intensity of α-TCP (1 3 2), (1 1 3) or (1 0 7) XRD lines at a determined time, t; $I_{\alpha,0}$ is the integrated intensity of α-TCP (1 3 2), (1 1 3) or (1 0 7) XRD lines at initial time (t = 0h); M_α is the is the mass absorption of α-TCP, 86.43 [40]; M_{CDHA} is the mass absorption of CDHA, 84.97 [40]; w_β is the mass fraction of ß-TCP during setting reaction; w_α is the mass fraction of α-TCP at a determined time, t and; $w_{\alpha,0}$ is the mass fraction of α-TCP at initial time (t = 0h). In this study, the external pattern method was employed [38]. The external pattern used in this work was β-TCP which is present in all samples and do not participate on the setting reaction, thus, its mass fraction is constant during all the process [5,39,40].

Moreover, the evolution of the specific surface area and the microstructure during the setting reaction was assessed by N_2 adsorption and scanning electron microscopy (SEM, JEOL-6400) respectively.

2.3 Statistics

One-way analysis of variance (ANOVA) and 2 sample t-tests were performed to compare differences between the mean values of samples' compressive strength using a confidence level of 95 %. In ANOVA analysis, Tukey's comparison post hoc test was performed to assess differences in each pair of means. Normality and equal variances tests were conducted

prior to ANOVA to guarantee that data followed Normal distribution and presented homoscedasticity.

3. Results and discussion

Figure 1 displays the XRD patterns of the synthesized TCP powders, which consist of almost pure α-TCP. Small amounts of β-TCP were also detected. The β-TCP content in α-TCP was 8 wt % and diminished to only 4 wt % in Si-α-TCP, thus confirming the efficacy of silicon doping in stabilizing the α-TCP crystalline phase, even at lower temperatures [27].

INSERT FIGURE 1

XRF results (Table 1) showed that in both Si-α-TCP and α-TCP the Ca/(P+Si) or Ca/P ratios were very similar to the expected ones, i.e. 1.5. Both TCP powders had very similar particle size distributions and specific surface areas as can be observed on Table 2. Hence, it would be expected that both powders presented similar kinetics during their setting reaction since, despite of Si addition, powders' physical properties (SSA, mean particle size and particle size distribution) did not present a significant difference [42–44].

INSERT TABLE 1

INSERT TABLE 2

Figure 2 shows the evolution of the XRD patterns with time. For both samples, α-TCP and hydroxyapatite were the main crystalline phases observed after different times of setting, confirming that the reaction consists on the dissolution of α-TCP particles and the precipitation of apatite crystals. In the case of Si-α-TCP cement, XRD peaks of apatite were only visible after 72 h, while for the α-TCP cement these peaks were already visible after 8 h. Moreover, the decrease on the diffraction lines intensities for both samples was very different. For instance, at 2 h of reaction, the (1 0 7) peak, i.e. the 100% relative intensity line for α-TCP (identified in Figure 2 by *), decreased its intensity around 30% for α-TCP, while it only decreased around 13% for Si-α-TCP. This discrepancy was observed during the entire setting

reaction, which was complete after 168 h for both cements. These results suggested that silicon substitution reduced the reaction kinetics of Si-α-TCP.

INSERT FIGURE 2

Figure 3 shows the conversion rate (α_t) for Si-α-TCP and α-TCP cements. The experimental values obtained for both samples fitted in agreement with a model proposed in the literature [39] for α-TCP cement (Equation 3). The time constant (k) was also normalized with the SSA (k_{SSA}) as shown in Table 3. Interestingly, k_{SSA} for Si-TCP (0.021 g.m^{-2}.h^{-1}) was almost four times lower than for α-TCP (0.072 g.m^{-2}.h^{-1}) confirming that Si reduces the velocity of the cement setting reaction.

INSERT FIGURE 3

$$\alpha(t) = 1 - e^{-kt}$$ **Equation 3**

INSERT TABLE 3

The kinetics of the cement reaction was also evaluated by measuring the evolution of the compressive strength with time (Figure 4) and the microstructure in the fracture surface (Figure 5). The compressive strength increased as the setting reaction evolved (Figure 4). The increase, especially for the first 72 h, was more pronounced for α-TCP than for Si-α-TCP. Whereas at 24 h α-TCP had already achieved 6 MPa, Si-α-TCP had only reached 0.6 MPa. Even though compressive strength evolution was slower for Si-α-TCP, it reached a significantly higher ($p < 0.05$) mechanical resistance than α-TCP at 168 h. For both materials the mechanical properties were enhanced as a result of the setting reaction evolution and the entanglement of apatite crystals. Unreacted α-TCP particles were observed for both samples during the initial 72 h (Figure 5 a-d). Furthermore, the apatite crystals formed surrounding the TCP particles during the setting reaction were bigger crystals in α-TCP than in Si-α-TCP. In

general, larger and lower amount of crystals have been ascribed to a lower number of nucleation points due to a lower degree of oversaturation in the cement paste [42,43,45]. However, in this case the smaller size of the crystals formed on the particles of Si-α-TCP could be ascribed to a higher oversaturation. This would be apparently in contradiction with the lower conversion rate observed for Si-α-TCP. These results could be explained by a competing mechanism occurring to Si-α-TCP. The presence of silicon could result in the formation of an amorphous silicate or silica gel on the surface of TCP crystals [28]. This amorphous layer could decrease the reactivity of the reagent by hindering the dissolution of α-TCP particles and therefore slowing down the precipitation and growth of apatite crystals.

INSERT FIGURE 4

INSERT FIGURE 5

The smaller size of the precipitated apatite crystals (Figure 5) for Si-α-TCP than for α-TCP at 168 h could explain the higher mechanical resistance ($p < 0.05$) for Si-α-TCP due to a more effective crystal entanglement with fewer pores entrapped between crystals. The mechanical properties achieved for both Si-α-TCP (12.80 ± 0.38 MPa) and α-TCP (11.44 ± 0.54 MPa) were low compared to the values reported on the literature, 20 MPa for Si-TCP [26,28] and 40 MPa for α-TCP [43]. The lower mechanical properties in the current study were ascribed to the higher liquid-to-powder ratio employed (0.6 mL.g^{-1}) which was needed in order to promote the ideal moldability of the CPC paste. Moreover, in contradiction with previous works [26,28], silicon did not reduce the final mechanical strength of the material but rather significantly increase it ($p<0.05$).

The difference on apatite crystals size was also observed by the evolution of SSA with time (Figure 6). At short times (4 and 8h), a smaller SSA was observed for Si-TCP than for α-TCP. The smaller SSA values observed at short times indicated a lower number of apatite crystals precipitated, which correlated well with the slower kinetics of Si-α-TCP observed by XRD. In

contrast, at longer times (168 and 450 h) a higher SSA was determined for Si-α-TCP than for α-TCP, in accordance with the size of the crystals observed by SEM (Figure 5).

INSERT FIGURE 6

In conjunction, the results showed that silicon substitution changed the reaction kinetics of α-TCP by reducing the material solubility [30]. The main reason for that could be the stabilization of the crystal structure provided by silicon substitution in some phosphate sites, leading to a structure with minor distortions [30,46]. These results were unexpected since other works performed with hydroxyapatite have indicated that Si distorted the crystalline structure and, therefore, increased the solubility of the end product [47].

The reason why Si slows down the reaction kinetics of α-TCP is still unclear. On one hand it could be speculated that during the dissolution and precipitation process that takes place, silicon may be involved in the formation of an amorphous silica gel on the surface of the TCP particles due to silicate ions liberation, as proposed by Hench in a well-accepted mechanism of biomineralization [48]. The formation of a silica-rich layer on the surface of the α-TCP could hinder its dissolution, delaying apatite precipitation and leading to a reduction on the setting reaction velocity [28,30]. To determine the mechanism by which Si alters the reactivity of α-TCP was out the scope of this work and should be studied in a future work.

4. Conclusion

Si-α-TCP was obtained with higher purity that its counterpart free of silicon (α-TCP). Both α-TCP and Si-α-TCP had similar particle size distributions and specific surface area. The evolution of the crystalline phases was evaluated when mixing the TCP compounds with water and the reactivity of Si-α-TCP was shown to be lower than that of α-TCP. Si-α-TCP produced a cement with higher mechanical properties which was ascribed to the smaller size of the entangled crystals. The smaller reactivity of Si-α-TCP could be due to the formation of an amorphous silicon layer hindering the dissolution of α-TCP particles and slowing down the reaction.

Acknowledgements

References

[1]   W.E. Brown, L.C. Chow, A New Calcium Phospate Setting Cement, J. Dent. Res. 62 (1983) 672–679.

[2]   R.Z. LeGeros, A. Chohayeb, A. Shulman, Apatitic Calcium Phosphate: Possible dental restorative materials, J. Dent. Res. 61 (1982) 343–347.

[3]   M.P. Ginebra, M. Espanol, E.B. Montufar, R.A. Perez, G. Mestres, New processing approaches in calcium phosphate cements and their applications in regenerative medicine., Acta Biomater. 6 (2010) 2863–73. doi:10.1016/j.actbio.2010.01.036.

[4]   M.-P. Ginebra, C. Canal, M. Espanol, D. Pastorino, E.B. Montufar, Calcium phosphate cements as drug delivery materials., Adv. Drug Deliv. Rev. 64 (2012) 1090–110. doi:10.1016/j.addr.2012.01.008.

[5]   E.B. Montufar, Y. Maazouz, M.P. Ginebra, Relevance of the setting reaction to the injectability of tricalcium phosphate pastes, Acta Biomater. 9 (2013) 6188–6198. doi:10.1016/j.actbio.2012.11.028.

[6]   P.M.C. Torres, S. Gouveia, S. Olhero, A. Kaushal, J.M.F. Ferreira, Injectability of calcium phosphate pastes: Effects of particle size and state of aggregation of β-tricalcium phosphate powders., Acta Biomater. (2015). doi:10.1016/j.actbio.2015.04.006.

[7]   S. Heinemann, S. Rössler, M. Lemm, M. Ruhnow, B. Nies, Properties of injectable ready-to-use calcium phosphate cement based on water-immiscible liquid., Acta Biomater. 9 (2013) 6199–207. doi:10.1016/j.actbio.2012.12.017.

[8]   R.G. Carrodeguas, S. De Aza, α-Tricalcium phosphate: synthesis, properties and biomedical applications., Acta Biomater. 7 (2011) 3536–46. doi:10.1016/j.actbio.2011.06.019.

[9]   M. Motisuke, R. García Carrodeguas, C.A.C. Zavaglia, Mg-Free Precursors for the Synthesis of Pure Phase Si-Doped α-Ca3(PO4)2, Key Eng. Mater. 361–363 (2008) 199–202. doi:10.4028/www.scientific.net/KEM.361-363.199.

[10]   J.W. Reid, K. Fargo, J.A. Hendry, M. Sayer, The influence of trace magnesium content on the phase composition of silicon-stabilized calcium phosphate powders, Mater. Lett. 61 (2007) 3851–3854. doi:10.1016/j.matlet.2006.12.046.

[11]   H.A.I. Cardoso, C.A.C. Zavaglia, Synthesis, characterization and reaction kinetics of high purity [alpha]-tricalcium phosphate, State University of Campinas, 2014.

[12]   J. Ando, Tricalcium Phosphate and its Variation, Bull. Chem. Soc. Jpn. 31 (1958) 196–201.

[13]   J.C. Araújo, M.S. Sader, E.L. Moreira, V.C. a. Moraes, R.Z. LeGeros, G. a. Soares, Maximum substitution of magnesium for calcium sites in Mg-β-TCP structure determined by X-ray powder diffraction with the Rietveld refinement, Mater. Chem. Phys. 118 (2009) 337–340. doi:10.1016/j.matchemphys.2009.07.064.

[14]   R. Famery, N. Richard, P. Boch, Preparation of α- and β-tricalcium phosphate ceramics, with and without magnesium addition, Ceram. Int. 20 (1994) 327–336. doi:10.1016/0272-8842(94)90050-7.

[15]   R.G. Carrodeguas, A.H. De Aza, X. Turrillas, P. Pena, S. De Aza, New Approach to the β→α Polymorphic Transformation in Magnesium-Substituted Tricalcium Phosphate and its Practical Implications, J. Am. Ceram. Soc. 91 (2008) 1281–1286. doi:10.1111/j.1551-2916.2008.02294.x.

[16]   R. Enderle, F. Götz-Neunhoeffer, M. Göbbels, F. a Müller, P. Greil, Influence of magnesium doping on the phase transformation temperature of beta-TCP ceramics examined by Rietveld refinement., Biomaterials. 26 (2005) 3379–84. doi:10.1016/j.biomaterials.2004.09.017.

[17]   R.G. Carrodeguas, A.H. De Aza, I. García-Páez, S. De Aza, P. Pena, Revisiting the phase-equilibrium diagram of the Ca3(PO4)2–CaMg(SiO3)2 system, J. Am. Ceram. Soc. 93 (2010) 561–569.

[18]   M. Motisuke, R.G. Carrodeguas, C.A. de C. Zavaglia, Si-TCP synthesized from "Mg-free" reagents employed as calcium phosphate cement, Mater. Res. 15 (2012) 568–572. doi:10.1590/S1516-14392012005000087.

[19]   M. Motisuke, R. García Carrodeguas, C.A.C. Zavaglia, A Comparative Study between α-TCP and Si-α-TCP Calcium Phosphate Cement, Key Eng. Mater. 396–398 (2009) 201–204. doi:10.4028/www.scientific.net/KEM.396-398.201.

[20]   F. W, H. H, H. R, Subsolidus relations in the system 2CaO.SiO2– 3CaO.P2O5, J. Am. Ceram. Soc. 52 (1969) 346–7.

[21]   N. RW, W. JH, G. W, High-temperature phase equilibria in the system dicalcium silicate–tricalcium phosphateitle, J. Chem. Soc. 220 (1959) 1077–83.

[22]   A.M. Pietak, J.W. Reid, M.J. Stott, M. Sayer, Silicon substitution in the calcium phosphate bioceramics., Biomaterials. 28 (2007) 4023–32. doi:10.1016/j.biomaterials.2007.05.003.

[23]   J.W. Reid, L. Tuck, M. Sayer, K. Fargo, J.A. Hendry, Synthesis and characterization of single-phase silicon-substituted alpha-tricalcium phosphate., Biomaterials. 27 (2006) 2916–25. doi:10.1016/j.biomaterials.2006.01.007.

[24]   I.M. Martínez, P. a. Velásquez, P.N. De Aza, Synthesis and stability of α-tricalcium phosphate doped with dicalcium silicate in the system Ca3(PO4)2–Ca2SiO4, Mater. Charact. 61 (2010) 761–767. doi:10.1016/j.matchar.2010.04.010.

[25]   M. I, S. JMS, G. IR, Synthesis and phase stability of silicate- substituted alpha-tricalcium phosphate, Key Eng. Mater. 361–363 (2008) 67–70.

[26]   G. Mestres, C. Le Van, M.-P. Ginebra, Silicon-stabilized α-tricalcium phosphate and its use in a calcium phosphate cement: characterization and cell response., Acta Biomater. 8 (2012) 1169–79. doi:10.1016/j.actbio.2011.11.021.

[27]   J.W. Reid, a Pietak, M. Sayer, D. Dunfield, T.J.N. Smith, Phase formation and evolution in the silicon substituted tricalcium phosphate/apatite system., Biomaterials. 26 (2005) 2887–97. doi:10.1016/j.biomaterials.2004.09.005.

[28]   C.L. Camiré, S.J. Saint-Jean, C. Mochales, P. Nevsten, J.-S. Wang, L. Lidgren, et al., Material characterization and in vivo behavior of silicon substituted alpha-tricalcium phosphate cement., J. Biomed. Mater. Res. B. Appl. Biomater. 76 (2006) 424–31. doi:10.1002/jbm.b.30385.

[29] R.G. Carrodeguas, A.H. De Aza, J. Jimenez, P.N. De Aza, P. Pena, A. López-Bravo, et al., Preparation and In Vitro Characterization of Wollastonite Doped Tricalcium Phosphate Bioceramics, Key Eng. Mater. 361–363 (2008) 237–240. doi:10.4028/www.scientific.net/KEM.361-363.237.

[30] X. Wei, O. Ugurlu, A. Ankit, H.Y. Acar, M. Akinc, Dissolution behavior of Si,Zn-codoped tricalcium phosphates, Mater. Sci. Eng. C. 29 (2009) 126–135. doi:10.1016/j.msec.2008.05.020.

[31] G. Mestres, C. Le Van, M.-P. Ginebra, Silicon-stabilized α-tricalcium phosphate and its use in a calcium phosphate cement: characterization and cell response., Acta Biomater. 8 (2012) 1169–79. doi:10.1016/j.actbio.2011.11.021.

[32] C. EM, Silicon : A Possible Factor in Bone Calcification, 1363 (1970) 4–5.

[33] L.T. Bang, K. Ishikawa, R. Othman, Effect of silicon and heat-treatment temperature on the morphology and mechanical properties of silicon - substituted hydroxyapatite, Ceram. Int. 37 (2011) 3637–3642. doi:10.1016/j.ceramint.2011.06.023.

[34] S. Bose, S. Tarafder, S.S. Banerjee, N.M. Davies, A. Bandyopadhyay, Understanding in vivo response and mechanical property variation in MgO, SrO and SiO_2 doped β-TCP., Bone. 48 (2011) 1282–1290. doi:10.1016/j.bone.2011.03.685.

[35] A.A.R.A.F. Khan, M. Saleem, A. Afzal, A. Ali, Bioactive behavior of silicon substituted calcium phosphate based bioceramics for bone regeneration., Mater. Sci. Eng. C. Mater. Biol. Appl. 35 (2014) 245–52. doi:10.1016/j.msec.2013.11.013.

[36] S. Sarda, E. Fernández, M. Nilsson, M. Balcells, J.A. Planell, Kinetic study of citric acid influence on calcium phosphate bone cements as water-reducing agent, J. Biomed. Mater. Res. 61 (2002) 653–659.

[37] E. Fernkdez, J.A. Planell, M.G. Boltong, M.P. Ginebra, O. Bermúdez, F.C.M. Driessens, Common Ion Effect on Some Calcium Phosphate Cements, 16 (1994) 99–103.

[38] B.D. Cullity, S.R. Stock, Elements of X-Ray Diffraction, Third Edit, 2001.

[39] M.P. Ginebra, E. Fernandez, E.A.P. De Maeyer, R.M.H. Verbeeck, M.G. Boltong, J.

Ginebra, et al., Setting Reaction and Hardening of an Apatitic Calcium Phosphate Cement, J. Dent. Res. 76 (1997) 905–912. doi:10.1177/00220345970760041201.

[40]   M.P. Ginebra, E. Fernandez, F.C.M. Driessens, J.A. Planell, Modeling of the hydrolysis of alpha-tricalcium phosphate, J. Am. Ceram. Soc. 82 (1999) 2808–2812.

[41]   E.C.S. Rigo, L.A. dos Santos, L.C.O. Verick, R.G. Carrodeguas, A.O. Boschi, α-Tricalcium Phosphate ans Tetracalcium Phosphate/Dicalcium Phosphate-based Dual Setting Cements, Lat. Am. Appl. Res. 37 (2007) 267–274.

[42]   M. Bohner, A.K. Malsy, C.L. Camiré, U. Gbureck, Combining particle size distribution and isothermal calorimetry data to determine the reaction kinetics of alpha-tricalcium phosphate-water mixtures., Acta Biomater. 2 (2006) 343–8. doi:10.1016/j.actbio.2006.01.003.

[43]   M.P. Ginebra, F.C.M. Driessens, J. a Planell, Effect of the particle size on the micro and nanostructural features of a calcium phosphate cement: a kinetic analysis., Biomaterials. 25 (2004) 3453–62. doi:10.1016/j.biomaterials.2003.10.049.

[44]   P.W. Brown, Effects of Particle Size Distribution on the Kinetics of Hydration of Tricalcium Silicate, J. Am. Ceram. Soc. 72 (1989) 1829–1832. doi:10.1111/j.1151-2916.1989.tb05986.x.

[45]   M. Espanol, R. a Perez, E.B. Montufar, C. Marichal, A. Sacco, M.P. Ginebra, Intrinsic porosity of calcium phosphate cements and its significance for drug delivery and tissue engineering applications., Acta Biomater. 5 (2009) 2752–2762. doi:10.1016/j.actbio.2009.03.011.

[46]   X. Wei, O. Ugurlu, M. Akinc, Hydrolysis of ?-Tricalcium Phosphate in Simulated Body Fluid and Dehydration Behavior During the Drying Process, J. Am. Ceram. Soc. 90 (2007) 2315–2321. doi:10.1111/j.1551-2916.2007.01682.x.

[47]   M. Vallet-Regí, D. Arcos, Silicon substituted hydroxyapatites. A method to upgrade calcium phosphate based implants, J. Mater. Chem. 15 (2005) 1509. doi:10.1039/b414143a.

[48]   L.L. Hench, Bioceramics: From Concept to Clinic, J. Am. Ceram. Soc. 74 (1991)

1487–1510. doi:10.1111/j.1151-2916.1991.tb07132.x.
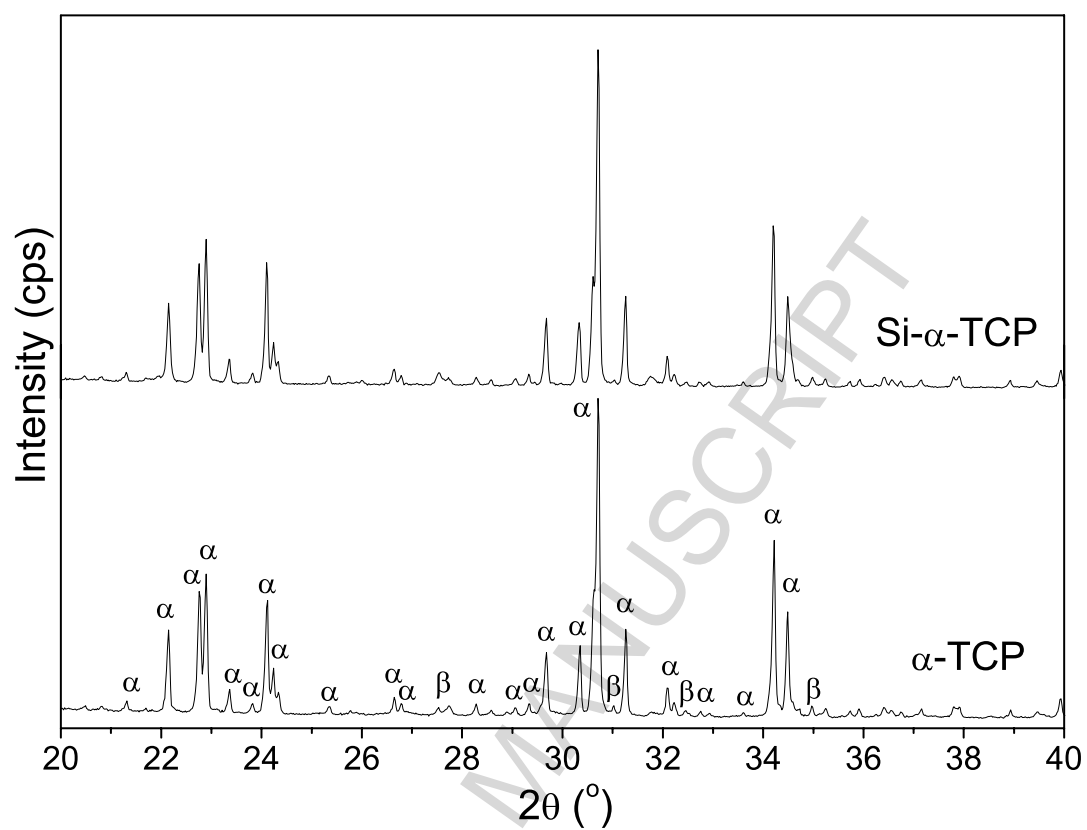
Figures Caption

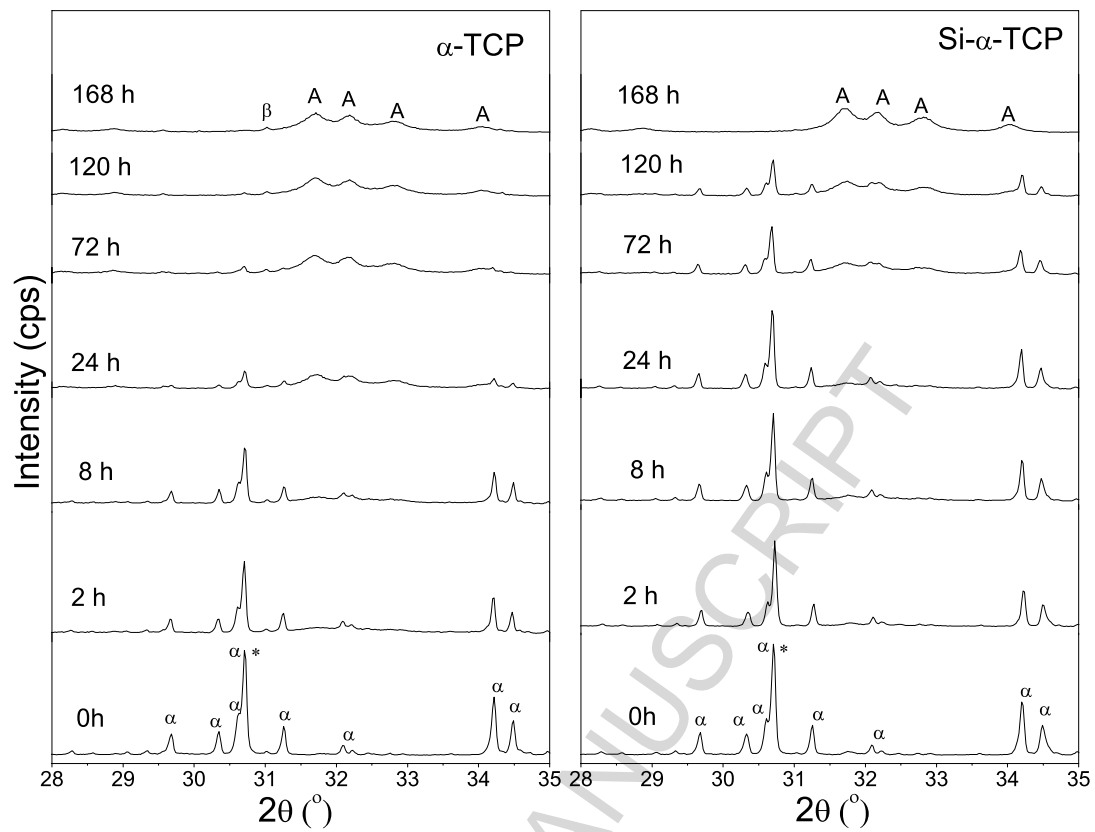**Fig. 1** XRD patterns of TCP powders. Legend: α = α-TCP.

Fig. 2 XRD patterns of the kinetics study for Si-α-TCP and α-TCP. Legend: α = α -TCP, ß = ß-TCP, A = apatite, * = (1 0 7) diffraction line of α-TCP.
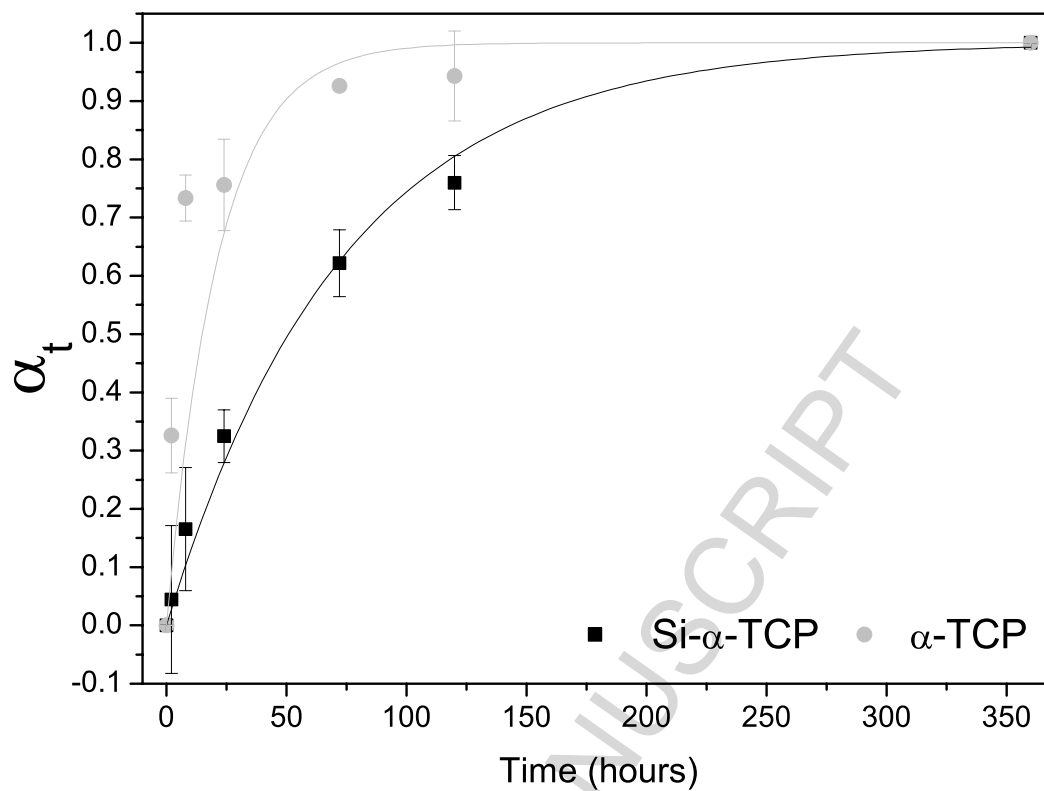
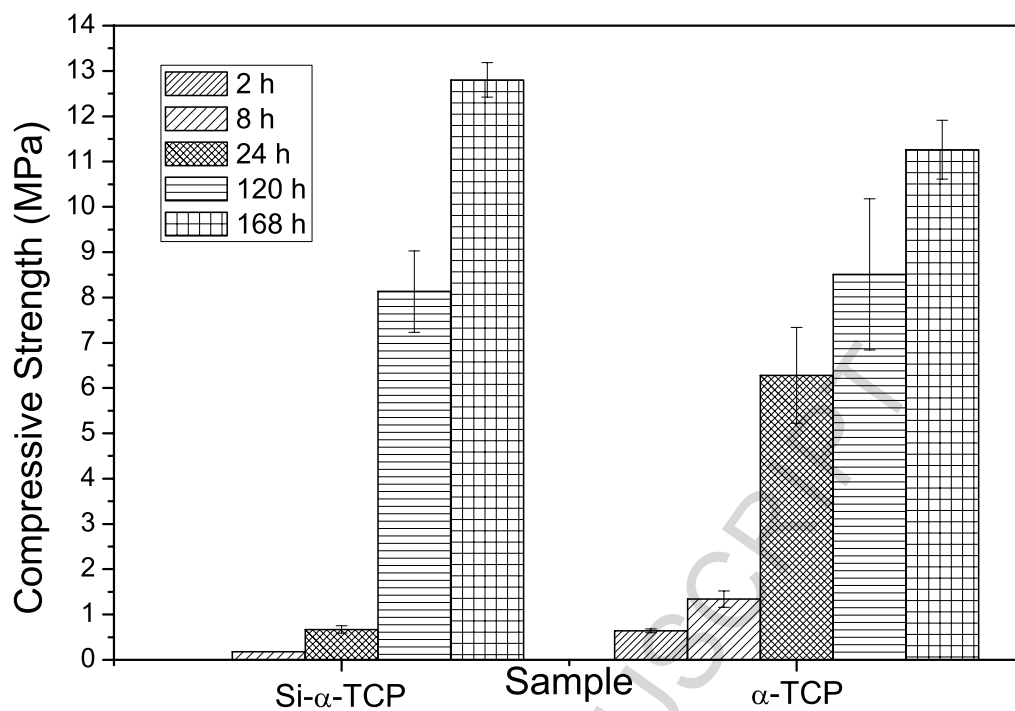**Fig. 3** TCP conversion (α_t) as a function of time.

Fig. 4 Evolution of compressive strength with time. The legends indicate the time points in hours.

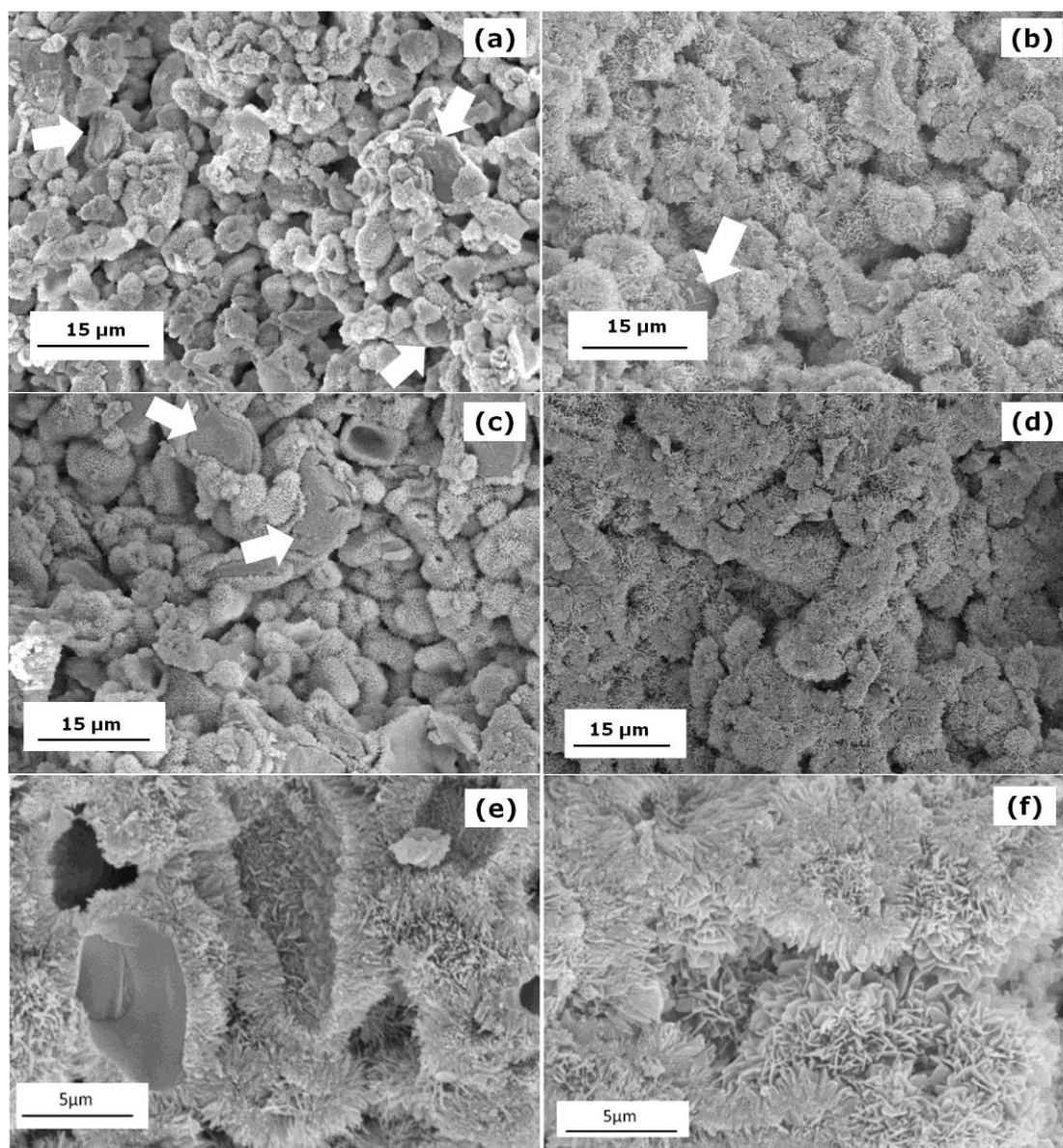**Fig 5** SEM micrographs of Si-α-TCP and α-TCP after: (a) Si-α-TCP 24 h; (b) α -TCP 24 h; (c) Si-α-TCP 72 h; (d) α -TCP 72 h; (e) Si-α-TCP 168 h and (f) α -TCP 168 h. The white arrows represent α-TCP or Si-α-TCP particles without reacting.
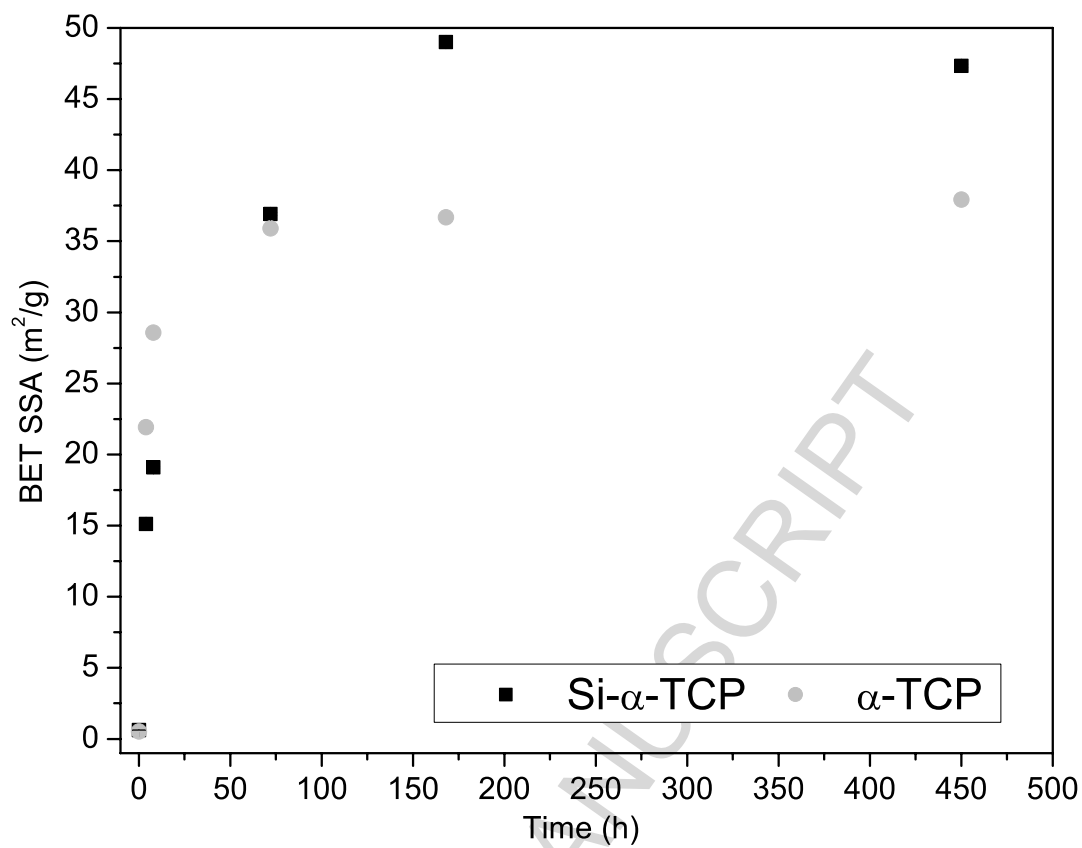
Fig. 6 Evolution of the SSA with time.

Tables

Table 1 XRF results. Ca/P and Ca/P+Si ratios. Values are in at.%

Sample	Ca	P	Si	Ca/P or Ca/(P+Si)
Si-α-TCP	22.89	14.60	1.04	1.46
α-TCP	23.08	15.38	---	1.50

Table 2 Specific surface area (SSA), mean particle size (d_{Mean}) and particle size distribution (10% < d < 90%).

Sample	SSA ($m^2.g^{-1}$)	d_{Mean} (µm)	10%<d<90% (µm)
α-TCP	0.5322 ± 0.0042	8.317	0.596<d<17.25
Si-α-TCP	0.6202 ± 0.0062	6.710	0.785<d<14.67

Table 3 Time constant (k) and time constant normalized by specific surface area (k_{SSA}) for Si-TCP and α-TCP.

Sample	k (h^{-1})	K_{SSA} ($g.m^{-2}.h^{-1}$)
Si-α-TCP	0.014 ± 1x10^{-3}	0.021
α-TCP	0.048 ± 4x10^{-3}	0.072

Highlights

- The influence of Silicon on α-TCP hydrolysis was investigated in this article

- Silicon reduced α-TCP reactivity by reducing its solubility

- Silicon has increased cement's mechanical resistance due to the smaller size of precipitated apatite crystals

- The formation of a silica-rich layer on the surface of the Si-α-TCP could hinder its dissolution, delaying apatite precipitation and leading to a reduction on the setting reaction velocity